Adv. Polar Upper Atmos. Res., **18**, 35–52, 2004

Cusp-latitude conjugate ionospheric absorption associated with increase of solar wind dynamic pressure during strong northward IMF—a case study

Masanori Nishino[1], Hisao Yamagishi[2], Natsuo Sato[2] and Ruiyuan Liu[3]

[1] *Solar-Terrestrial Environment Laboratory, Nagoya University, 3–13, Honohara, Toyokawa 442-8507*
[2] *National Institute of Polar Research, Kaga 1-chome, Itabashi-ku, Tokyo 173-8515*
[3] *Polar Research Institute of China, 451 Jinqiao Road, Pudong, Shanghai, 200129, China*

(Received December 19, 2003; Accepted April 1, 2004)

Abstract: Conjugate ionospheric absorption was observed in the magnetic pre-noon by the inter-hemispheric imaging riometers (IRISs) at Ny-Ålesund (NAL), Svalbard and Zhongshan (ZHS), Antarctica in the cusp-latitude. The absorption was associated with increase of solar wind dynamic pressure during the strong northward interplanetary magnetic field. The conjugate absorption features showed a sequence of spike-shape with intensity of <1 dB and duration time of 5–10 min, and also showed a large spatial extension (>400 km) exceeding the IRIS field-of-view with a poleward motion. The absorption spikes at NAL preceded the ones at ZHS by about 4 min. The absorption at NAL was located at part of enhanced auroral luminosity in the main oval from the POLAR UVI images, and also near the lower-latitude convection reversal in the plasma convection cell from the SuperDARN radar network of the northern hemisphere. Conjugate relationships, electrodynamics of electron precipitation and possible absorption mechanisms are discussed from these characteristics.

key words: conjugate absorption, northward IMF, solar wind pressure increase

1. Introduction

Dynamical phenomena at the dayside magnetopause like upstream solar wind dynamic pressure and magnetic reconnection have been much attracted recently for understanding interaction between solar wind and magnetosphere. Glassmeier and Heppner (1992) considered theoretical models of a spatially localized pressure pulse and localized magnetic field merging at the dayside magnetopause in relation to traveling magnetospherc convection twin vortices.

Paying an attention to specific changes in solar wind dynamic pressure, Sibeck *et al*. (1989a) revealed that the magnetospheric response to upstream solar wind dynamic pressure oscillations has been identified as quasi-periodic variations in electron precipitation by riometer absorption, high-latitude ground magnetic pulsations and ELF-VLF radio wave emissions near local magnetic noon at South Pole (geomagnetic latitude, 75°S) when the interplanetary magnetic field (IMF) pointed nearly radially toward the Sun. Sibeck *et al*. (1989b) also have revealed that some transient ground magnetic events near dawn at South

Pole are related to variations in solar wind dynamic pressure and not necessarily to magnetic merging at the dayside magnetopause. Farrugia *et al*. (1989) demonstrated ground magnetic signatures for sudden changes in the solar wind dynamic pressure during a strong northward IMF. They have suggested that magnetic reconnection-related coupling is unlikely a priority. Sandholt *et al*. (1994) examined cusp/cleft auroral activities in the pre-noon time in relation to changes in solar wind dynamic pressure and IMF variability. Farrugia *et al*. (1995) demonstrated transient auroral activities in the post-noon at Ny-Ålesund (geomagnetic latitude, 76.1°N) stimulated by the arrival at Earth of upstream dynamic pressure pulses while the IMF was aligned in a Parker spiral direction with IMF $B_y \ll 0$ and small or zero B_z. They revealed that the transient aurora came from the cusp and near cusp, but the persistent aurora consisted mainly of low-latitude boundary layer (LLBL) precipitation on closed magnetic field lines. Sandholt *et al*. (1996) examined cusp/cleft auroral forms and activities due to particle precipitation responding to specific changes in solar wind and IMF conditions in relation to ionospheric convection.

As described above, the magnetospheric response and associated ionospheric signatures in the cusp/cleft ionosphere are very complicated for the arrival at Earth of upstream dynamic pressure pulses under the variability of the IMF conditions. Therefore, to examine whether ionospheric signatures come from the dayside magnetosphere on closed or opened magnetic field lines is a clue for understanding dynamical interaction at the dayside magnetopause. In the auroral region, conjugate observations of auroral luminosity between the inter-hemispheric stations have been carried out in limited periods near equinox (*e.g.* Sato *et al*., 1998), however, it is quite impossible between the inter-hemispheric stations in the cusp latitude due to the opposite condition of sunlight.

In earlier years, conjugate observations of riometer absorption have been carried out between the inter-hemispheric stations in the cusp latitude using a single broad-beam antenna (Hargreaves and Chivers, 1965). Thereafter, an imaging riometer (IRIS) was first developed at South Pole (Detrick and Rosenberg, 1990). The IRIS is the most powerful and available means instead of the auroral image observations. Nishino *et al*. (2000) first reported conjugate daytime absorption events using the three IRISs ($L = 14$–20) at Ny-Ålesund in Svalbard, Danmarkshavn in Greenland and Zhongshan in Antarctica (see Fig. 1 below). They found a conjugate absorption feature of an eastward moving small spatial-scale (< 100 km) in the magnetic post-noon, which was associated with a steep increase of the solar wind dynamic pressure and the simultaneous short-period southward IMF change. They have indicated that magnetospheric electrons drifting eastward from the nightside magnetosphere are stimulated by high dynamic pressure of the solar wind. However, it is still unclear whether the stimulation occurs on closed or opened magnetic field lines at the dayside magnetopause.

In this study, we examine a pre-noon absorption event on August 26, 1998 observed by the inter-hemispheric cusp-latitude IRISs at Ny-Ålesund and Zhongshan. The absorption event was associated with increase of solar wind dynamic pressure during a strong northward IMF for which stimulation would occur on closed magnetic field lines. First we present conjugate absorption features, and discuss a conjugate relationships, electrodynamics of electron precipitation and possible absorption mechanisms, combining with simultaneous data of the POLAR-satellite UVI images, DMSP-satellite particles, SuperDARN plasma convection.

2. Inter-hemispheric cusp-latitude IRISs

Table 1 shows geophysical coordinates of the two IRIS stations, Ny-Ålesund (NAL), Svalbard and Zhongshan (ZHS), Antarctica that we use in this study, and their corrected geomagnetic latitudes, approximate magnetic noon and total magnetic field intensities according to the IGRF model.

Figure 1 shows the location of NAL (L~16) and an approximate field-of-view (FOV) of the IRIS with invariant latitude contours for 70° and 80° in the European arctic region. Curves giving magnetic conjugate locations of ZHS (L~14) are drawn for the time-periods of 02–08 UT and 14–19 UT in the northern summer solstice (June 20) (modified from Yamagishi *et al*., 1998), based on the calculations using Tsyganenko 1996-model. The cal-

Table. 1. Geophysical coordinates of the two IRIS stations, Ny-Ålesund (NAL), Svalbard and Zhongshan (ZHS), Antarctica, and their corrected geomagnetic latitudes, approximate magnetic noon and total magnetic field intensities according to the IGRF model.

Station name (Acronym)	Geographical coordinates	Corrected geomagnetic latitude	Eccentric dipole magnetic noon	Total magnetic field
Ny-Ålesund (NAL)	78.92N, 1.92E	76.05N	0847 UT	53959 nT
Zhongshan (ZHS)	69.37S, 6.38E	74.52S	1015 UT	53733 nT

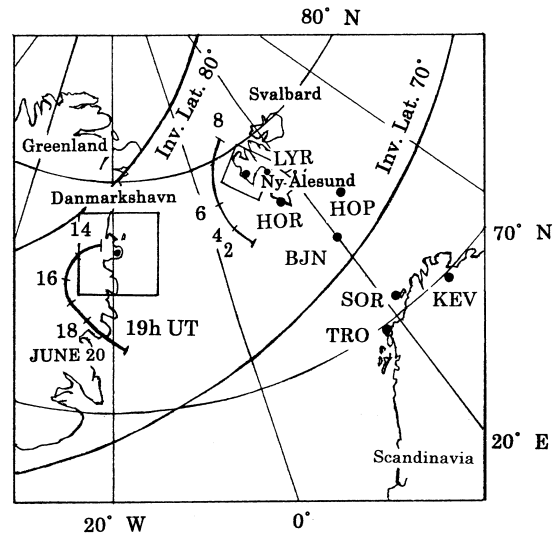

Fig. 1. Location of NAL (L~16) and an approximate field-of-view of the IRIS with invariant latitude contours for 70° and 80° in the European arctic region. Curves giving magnetic conjugate locations of Antarctic ZHS (L~14) are drawn for the time-periods of 02–08 UT and 14–19 UT in the northern summer solstice (June 20) based on the calculations using Tsyganenko 1996 model (modified from Yamagishi et al., 1998). The IMAGE magnetometer chain stations extending from Svalbard to northern Scandinavia are also noted by acronyms.

culations are performed under the IMF-$B_y = B_z = 0$ conditions. For other time-periods, no conjugate location is obtained due to opened magnetic field line configurations. It is found that the magnetic conjugate locations of ZHS are obtained at the western region near Svalbard in the morning and around the eastern coast of Greenland in the afternoon.

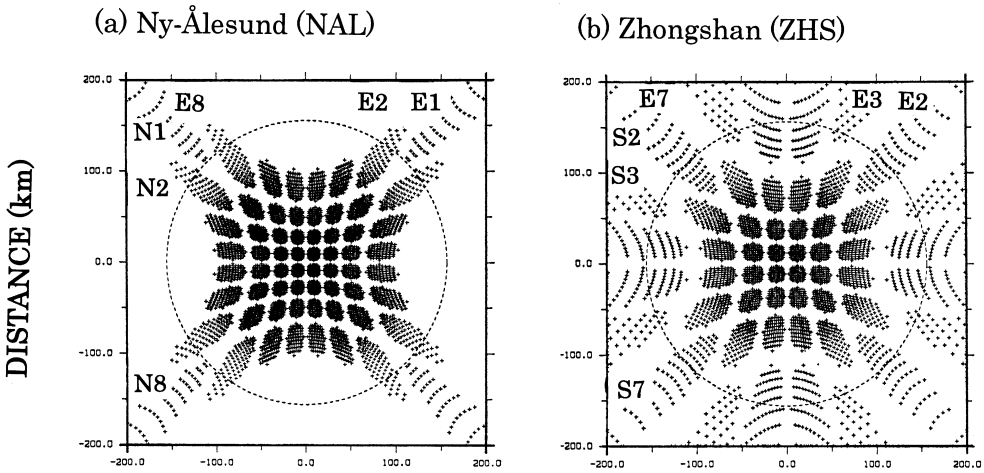

Fig. 2. Projection of two-dimensional 8 × 8 half-power beam-widths onto the ionospheric absorption layer at 90 km altitude for the two IRISs. Left panel shows the beam pattern for NAL, in which the beam numbers are assigned for north-to-south (N1, , , N8) and for east-to-west (E1 , , , , E8) orientations. Right panel shows the beam pattern for ZHS, in which the beam numbers are assigned for south-to-north (S2 , , , S7) and east-to-west (E2, , , ,E7) orientations (modified from Yamagishi et al., 1992).

Figure 2 shows the projection of two-dimensional 8 × 8 half-power beam-widths onto the ionospheric absorption layer at 90 km altitude for the two IRISs (modified from Yamagishi *et al*., 1992). Left part shows the beam pattern for NAL, in which the beam numbers are assigned for north-to-south (N1, , , N8) and for east-to-west (E1, , , , E8) orientations. Most beams except corners are included in a 200 km × 200 km square, which is defined as the NAL-FOV. Right panel shows the beam pattern for ZHS, in which the beam numbers are assigned for south-to-north (high-to-low latitudes) (S2, , , S7) and east-to-west (E2, , , E7) orientations. Most beams except corners are included in a 400 km × 400 km square, which is defined as the ZHS-FOV. The north-south beams on the both IRISs are aligned to the invariant north-south direction.

Ionospheric absorption of cosmic radio noise is usually obtained by subtraction between decreased cosmic radio noise intensities and background cosmic radio noise level (quiet-day-curve, QDC) in absence of absorption. Absorption calculations for the IRIS are executed for all of the two-dimensional 8 × 8 beams. Technical performances and data processes on the IRIS system were reported by Yamagishi *et al*. (1992) and Sato *et al*. (1992), respectively, and the initial observation results at NAL were presented by Nishino *et al*. (1993).

3. Conjugate features of pre-noon absorption

Figure 3 shows time variations of the IMF-B_x, -B_y and -B_z components and ion dynamic pressure of solar wind during 00–12 UT on August 26, 1998 from the WIND spacecraft, which are used for studies of conjugate absorption features. The WIND was located at about 118 R_e upstream of the Earth during the time period. The solar wind pressure persisted with 2–3 nPa and the IMF directed mainly duskward with small changes of northward and southward until about 0635 UT. The solar wind pressure suddenly and impulsively increased to ~16 nPa at 0636 UT, and thereafter decreased gradually from ~10 nPa to ~5 nPa, showing small peaks with 30–60 min durations until 12 UT. Synchronized with the impulsive increase of the solar wind pressure at 0636 UT, the IMF B_x showed a sharp negative excursion (~15 nT) followed by a positive impulse, and thereafter showed fluctuations

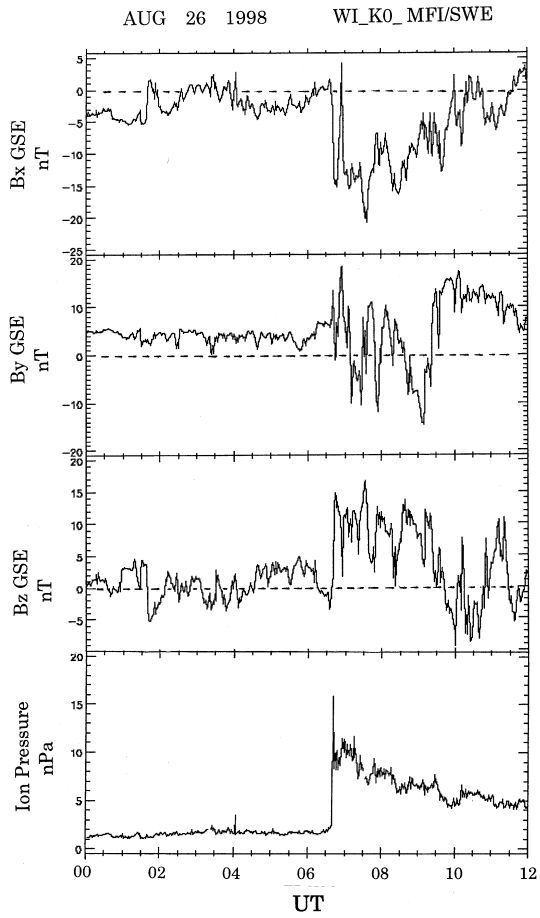

Fig. 3. Time variations of the IMF-B_x, -B_y and -B_z components and ion dynamic pressure of solar wind during 00–12 UT from the WIND spacecraft.

with negative values. The IMF B_y showed a positive impulse, followed by fluctuations with large positive/negative excursions. It should be noted that the IMF B_z showed pulsating variations with large positive values until about 0940 UT. In this study, we examine the absorption event associated with the increase of solar wind dynamic pressure during the strong northward IMF between 0636 UT and 0940 UT.

Figure 4 shows time variations of ionospheric absorption in the north-south beams (N1–N8) on the western beam (E＝7) for NAL and the south-north beams (S1–S8) near the zenith (E＝4) for ZHS during 02–04 UT and 06–11 UT. The scale of absorption intensity is 4 dB/div for the both stations. At the upper part in this figure, the time variation of solar wind dynamic pressure is depicted with delay time of 16 min. The delay time is estimated from propagation delay from satellite to the bow shock and from the bow shock to the polar ionosphere through the dayside magnetopause. The WIND satellite was located at about 118 R_e upstream, and the solar wind attained to high-speed of about 690 km/s during the time period. Assuming that the position of the bow shock is 12 R_e (Stauning *et al*., 1995), the propagation delay between the WIND and the shock is estimated to be 16.3 min. Adding the propagation delay from the bow shock to the polar ionosphere, total delay may be longer than 16.3 min. However, as this estimation includes ambiguities, we here use the delay time between the pressure impulse (0636 UT) on the WIND and the sudden commencement (0652 UT) of the magnetic variation at the low-latitude Kakioka station (36.2°N, 140.2°E).

Associated with the steep increase of the solar wind dynamic pressure and synchronized discontinuity in the IMF orientation at 0636 UT, the absorption at NAL increased in all the north-south beams, attained to a first spike-shape just before 0700 UT, and subsequently attained to a second one near 0716 UT, followed by small spikes around 0730 UT, 0800 UT and 0950 UT. The absorption at ZHS showed a first spike just after 0700 UT (small step-absorption at the S1-beam just before 0700 UT was contaminated by interference radio noise), and followed by some absorption spikes near 0720 UT, 0734 UT, 0804 UT and 0954 UT. Here it should be noted that these absorption spikes at the both stations were superposed to polar cap absorption (PCA) of about 3 dB intensity started at about 0205 UT on August 26 which is shown at the left part of the absorption variations. Thus, net intensity of the absorption spikes is less than 1 dB. It should be remarked that these absorption spikes correspond to the impulsive increase (0636 UT) and subsequent small increases (~0658 UT, ~0714 UT and ~0744 UT at the WIND time) of the solar wind dynamic pressure during the strong northward IMF. Another remarkable feature in Fig. 4 is that the absorption spikes at NAL preceded the ones at ZHS by about 4 min.

The upper and lower panels of Plate 1 show time-series of absorption image data with a 256 s integration period during about 0654–0754 UT at NAL and ZHS, respectively. The absorption image data are composed from the two-dimensional 8×8 beam data by the algorithm of interpolation and extrapolation (Sato *et al*., 1992). For NAL, up is northward (poleward) and right is westward, while for ZHS, up is southward (poleward) and right is eastward. The absorption intensity is displayed by color codes in the range of 0–6 dB below the image data. It is found from the image data for NAL that the background PCA (~3 dB) is uniformly expanded in the whole FOV, as displayed by light blue, and the superposed absorption-spikes (yellow/red colors) are distributed nearly in the whole FOV, although the absorption intensities are largely decreased at the central southern-part because of abnormal

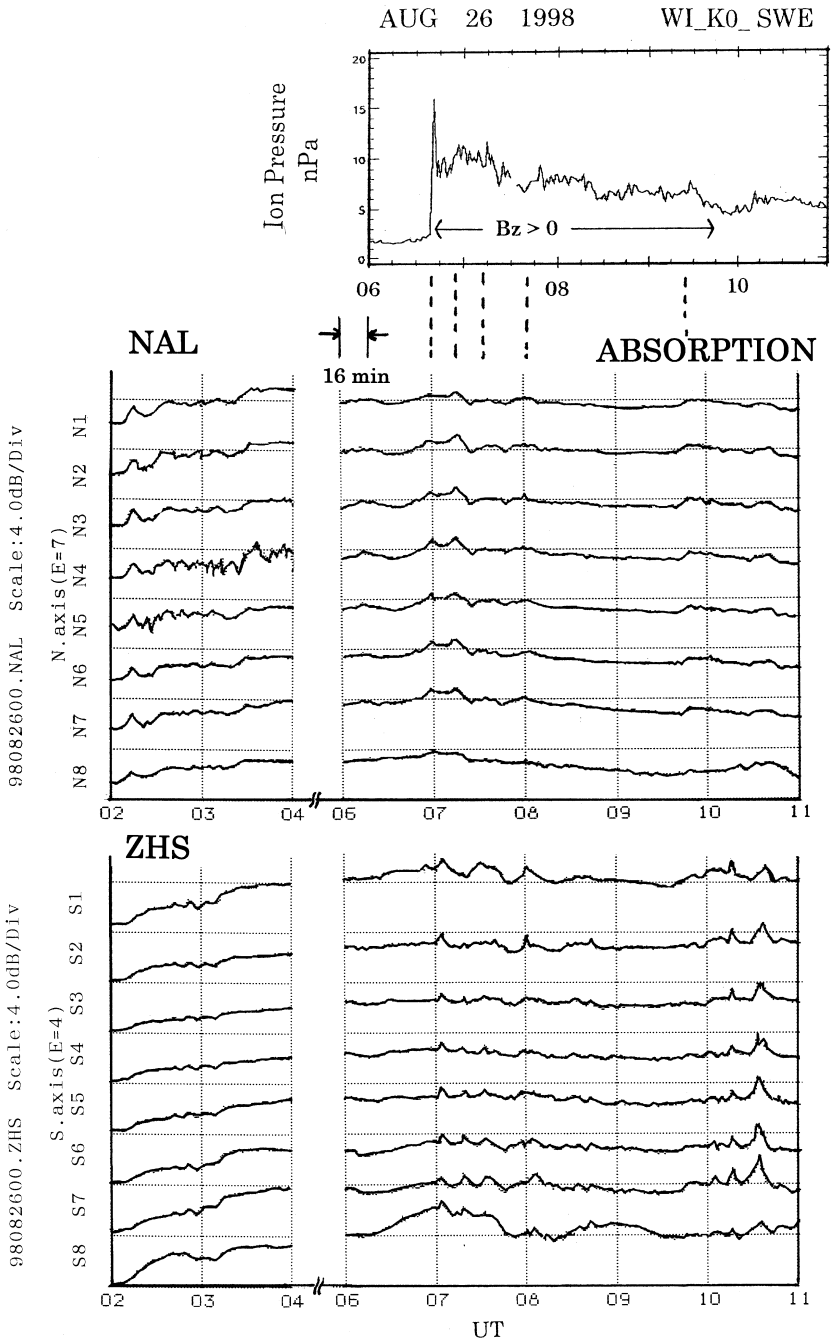

Fig. 4. Time variations of ionospheric absorption in the north-south beams (N1–N8) on the western beam (E=7) at NAL and the south-north beams (S1–S8) near the zenith (E=4) of ZHS in the time period of 02–11 UT. The scale of absorption intensity is 4 dB/div for the both stations. In the upper panel, the time-variation of the solar wind pressure is displayed with delay time of 16 min.

high-QDC values due to strong local interference noise. Consequently the absorption spikes are likely expanded to larger area exceeding the FOV showing a little enhancement at the western part in the FOV.

On the other hand, it is found from the absorption image data for ZHS that the background PCA is displayed with enhancement like a ring of about 100 km radius surrounding the zenith (red/green color-codes). This is caused by the non-identical beam projections onto the ionosphere level, as seen in Fig. 2, and the algorithm of the image composition. The corner beams occupy relatively larger areas, resulting that their absorption intensities are apparently strengthened comparing to those near the zenith. Therefore, it is difficult to identify the image enhancement corresponding to the absorption spikes. However, looking at distribution plots of the absorption intensities (intensity variations on the two-dimensional 8×8 beams with time), the absorption spikes are expanded in the whole FOV showing enhancement at the southern part (high-latitude part) in the FOV. Consequently the absorption spikes are likely expanded to larger area exceeding the FOV, as well as the case for NAL.

The left and right panels of Fig. 5 show time-expanded absorption variations in the east-west and north-south beams during about 0630–0800 UT for NAL and ZHS, from which motion of the absorption spikes are examined. The variations at the outermost beams are excluded because of the strong contamination. It is found that the first and second absorption spikes shown by broken lines represent pronounced poleward motions (~2.0 km/s) for the both stations, but include the motion of an eastward component (~1 km/s) for only ZHS.

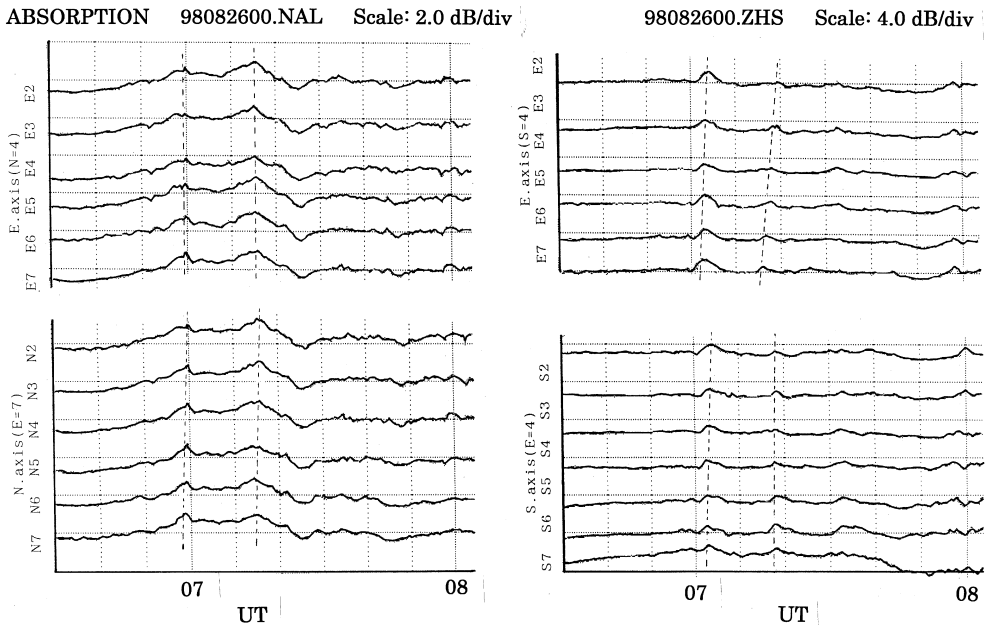

Fig. 5. Time variations of the absorption in the east-west and north-south beams during 0630–0800 UT at NAL (left) and ZHS (right).

4. Summary and discussion

The pre-noon absorption spikes presented in this study were associated with the increase of solar wind dynamic pressure during the strong northward IMF, and showed some interesting conjugate features, as follows.

1) The absorption spikes showed the intensity less than 1dB and the duration of 5–10 min.
2) The absorption spikes at NAL preceded the ones at ZHS by about 4 min.
3) The absorption spikes showed larger area exceeding the IRIS-FOV.
4) The absorption spikes showed the poleward motion.

In early years, Brown (1973) showed a sudden commencement absorption event in the post-noon at South Pole (74.2° invariant latitude) after prolonged magnetic quiet. Brown (1977) also showed the presence of sudden commencement absorption from the riometer records at Godhavn, Greenland (77.2° invariant latitude), which occurred in the post-noon during quiet geomagnetic conditions when the IMF was northward. He has revealed that the event is consistent with the last closed magnetic field lines coinciding with the equatorward boundary of the cusp.

In this section, we discuss the conjugate features described above with regards to conjugate relationships and electrodynamics of electron precipitation and possible absorption mechanisms.

4.1. Conjugate relationship

Nishino *et al*. (2000, 2001) demonstrated the conjugate absorption spikes near 12 UT (~15 MLT) in August between NAL and ZHS, associated with the dynamic pressure increase of the solar wind. The absorption spikes showed small spatial scale (~100 km) at the western part of the zenith in the FOV at the both stations. They explained that the conjugate location of ZHS could be displaced to lower-latitudes than the calculated conjugate points due to the pressure increase and the synchronized southward change of the IMF.

Nishino *et al*. (2000) also demonstrated the conjugate absorption spikes near 10 UT (~13 MLT) in November between NAL and ZHS, associated with the sudden increase of the solar wind dynamic pressure. The absorption spikes showed larger spatial scale with east-west extension of several hundred km. The IMF swung to the southward immediately after the short-time northward excursion (~5 nT). Therefore it is difficult to discuss which factors of the IMF and/or the solar wind pressure affect the displacement of the conjugate points.

The calculated conjugate points of ZHS are situated at the western region near Svalbard in the time-period of 07–09 UT (see Fig. 1). In this study, we have demonstrated the absorption at NAL extending to larger area exceeding the FOV with enhancement at the western part, and also demonstrated the absorption at ZHS extending to larger area exceeding the FOV with enhancement at the high-latitude part, associated with the pressure increase of the solar wind during the strong northward IMF. Therefore it should be considered that the conjugate relationship is consistent with the calculations, particularly for the absorption enhancement parts between the inter-hemispheric stations. This result is significantly resulted from the conjugate IRIS observations under the strong northward IMF condition. It is thus concluded that perturbations at the dayside magnetopause could occur in the closed magnetic field lines connecting inter-hemispheric stations and the conjugate

locations are not largely displaced in latitudes and longitudes.

In the following, we briefly discuss the 4-min time precedence of the absorption spikes at NAL from the ones at ZHS, as shown in Fig. 4. This time precedence suggests that the solar wind pressure pulses could generate perturbations at the northern hemisphere side from the magnetic equator at the dayside magnetopause.

Hargreaves and Chivers (1965) analyzed statistically time difference of conjugate nighttime absorption events between Frobisher Bay (L~14) and South Pole (L~15). The occurrence number of the conjugate absorption showed a dominant peak in ± 5 min in time difference. They have considered that the time difference is caused by seasonal changes on the distance between anti-solar point and the magnetic equator on the nightside magnetic field lines, and calculated time difference of 4–8 min for the average $L = 14$ in northern summer, assuming hydromagnetic velocities of 320–640 km/s along the dipole magnetic field line. Nishino *et al*. (2000) observed the 1-min precedence at ZHS than at NAL for the conjugate afternoon absorption spikes in August. Recently Christensen *et al*. (2003) observed the time precedence of < 1 min at South Pole than at its conjugate point, Iqualuit in Canada (geomagnetic lat., 73°N) for the conjugate morning absorption in August.

Since the magnetic field configuration in the magnetosphere varies complicatedly depending on the IMF orientation, solar wind parameters, season and time, we have to analyze many conjugate absorption events. However, the present time precedence of the 4-min seems to be reasonable, referring to the calculations by Hargreaves and Chivers (1965).

4.2. Electron precipitation

Milan *et al*. (2000) demonstrated a sequence of auroral luminosity from the ultra violet imager (UVI) onboard Polar satellite of the northern hemisphere. Figure 6 shows part of the dayside auroral UV images during the present absorption event on August 26, 1998 in magnetic latitude (MLAT) and magnetic local time (MLT) in the polar coordinates; the latitudes shown are 70° and 80°, and 12 MLT toward the top of each panel, with 06 MLT and 18 MLT at the bottom right and left corners, respectively. The image data were acquired using LBH filter (140–160 nm) with a 36 s integration period approximately every 3 min (Torr *et al*., 1995). At 0719:42 UT when the second absorption spike was observed, enhancements of auroral luminosity (green color) are seen within the dayside main oval (blue color) in the pre-noon (panel a). The IRIS FOV at NAL (a white square in panel e) was situated near the lower-latitude boundary in the main oval. This suggests the presence of auroral electron sources on the closed magnetic field lines. Thereafter auroral luminosity in the pre-noon decreased with time, as seen from the following panels. Milan *et al*. (2000) studied mainly a poleward progressive auroral image with strong flux detached from the afternoon main oval, and interpreted this as the ionospheric footprint of a high-latitude reconnection site, combining with the velocity data from CUTLASS Finland radar scans. However, the poleward progressive aurora is outside of the IRIS FOV at NAL, which is out of scope of this study.

During the present absorption event, the DMSP satellite flew over the eastern area of Russia at 0710:00 UT, and approached to the eastern coast near Svalbard at 0718:00 UT after passing through the arctic sea. Plate 2 shows spectrograms of energetic particle (electrons and ions) precipitation with UT, MLAT, GLAT, GLONG and MLT on August 26, 1998. At 0718:00 UT on the second absorption spike, shown by an upward arrow, energy

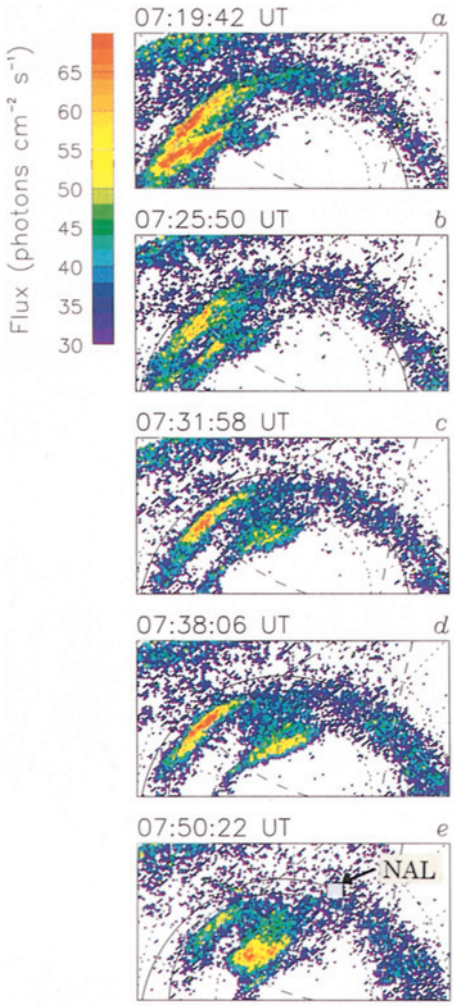

Fig. 6. Auroral UV images during the present absorption event on August 26, 1998 in magnetic latitude (MLAT) and magnetic local time (MLT) in the polar coordinates; the latitudes shown are 70° and 80°, and 12 MLT toward the top of each panel, with 06 MLT and 18 MLT at the bottom right and left corners, respectively (after Milan et al., 2000).

spectrum showed electron precipitations with strong fluxes (~10^{10} electrons) of the average energy of $<$ 1 keV and weak fluxes (~10^{8} electrons) extended up to 2 keV. The criterion based on plasma characteristics identifies the lower latitude boundary layer (LLBL) in the magnetosphere (Newell and Meng, 1992). Thus the pre-noon absorption spikes could be caused by precipitation of energetic electrons ($<$ 2 keV) from the LLBL into the *E*-region ionosphere in the main oval.

Sandholt *et al*. (1996) observed a transient discrete auroral form in 557.7 nm (green line) in the pre-noon (~09 MLT) at Ny-Ålesund at the time of the arrival of the interplanetary shock during the northward IMF ($<$ 10 nT). The intensity of the auroral emissions was 2–3 kR. The aurora appeared at the equatorward boundary of the preexisting cleft aurora, which covered the whole field of view of the auroral TV camera in the east-west direction. They have interpreted that the auroral signatures reflect plasma entry by magnetic reconnec-

tion at the lower latitudes (subcusp).

Sandholt *et al*. (2000) also observed green-line emissions of aurora during strongly northward IMF ($B_z = 7$ nT) after a rapid northward turning. The emissions were accompanied by an enhancement of the solar wind dynamic pressure from 2 to 5 nPa. Auroral activity showed a characteristic of an initial 1–2 min poleward step at the auroral poleward boundary. They have speculated that the green-line emissions are electron precipitations associated with lobe and low-latitude reconnections.

Although the solar wind and IMF conditions by Sandholt *et al*. are not quite coincident to the ones for the present absorption event, the present absorption could be caused by electron precipitation (< 2 keV) from the LLBL on the closed magnetic field lines. Newell and Meng (1994) revealed that high solar wind pressure (> 4 nPa) plays a crucial role in interaction of solar wind with the magnetosphere, regardless of the original IMF strength, and showed an extension of the LLBL to the lower-latitude side of the cusp. This result sustains the present absorption event caused by electron precipitation from the LLBL associated with the increase of the solar wind dynamic pressure.

4.3. Absorption mechanism

Stauning and Rosenberg (1996) analyzed statistically characteristics of noontime absorption spikes observed at the cusp-latitude IRIS station in Sondre Stromfjord (73.7° invariant latitude), Greenland. They have revealed that the noontime absorption spikes have the amplitudes of 0.2–0.3 dB at 38.2 MHz, the durations of 1–2 min, and limited region of typical dimensions of 50–100 km. Common to all cases were the negative average level (southward) of IMF-B_z. From the comparison with the polar ionospheric convection, they revealed that the noontime absorption spikes could occur at or within a few degrees of the equatorward of the convection reversal boundary at the afternoon convection cell. They have further suggested that the absorption spikes are related to the sudden precipitation of high-energy (30–300 keV) magnetospheric electrons, acting through near-saturated upward region 1 field-aligned-currents (FAC) at the afternoon convection reversal. However, the present absorption in this study may be a combination of the two types; sudden commencement absorption (SCA) and fluctuating daytime absorption (FDA) (Stauning, 1996) for which mechanism is not yet known.

Here we show ionospheric plasma convection patterns obtained simultaneously by SuperDARN HF radar network (Ruohniemi and Baker, 1998). Plate 3 shows flow vector plots in northern polar region during 2 min from 0658 UT, 0700 UT, 0714 UT, 0716 UT, 0732 UT and 0734 UT (approximately 1030–1100 MLT) when the absorption spikes were observed. The vectors are plotted in MLT/MLAT coordinates. At the right-down corner of the coordinates the IMF orientation is displayed in the *X-Y* plane in the precedence of 16 min from the SuperDARN time. The NAL-FOV is marked at the 76° MLAT in the first pattern. At 0654 UT before the absorption onset, the velocity of flow vectors is < 200 m/s in the pre-noon (not shown here). At 0658 UT when the first absorption spike was observed, the velocity increased to ~600 m/s, and at 0700 UT the vectors changed to poleward (anti-sunward) near the convection reversal of the enhanced convection cell in the noon sector. This change could be caused by the impulsive increase of solar wind dynamic pressure. Different convection flows are simultaneously enhanced with higher velocity (~2000 m/s) at the high-latitude edge of the morning convection cell, which is far from the NAL-FOV.

During 0714–0718 UT while the second absorption spike was observed, the flow vectors moved poleward with the westward direction in the lower-latitude part of the convection cell, which fact could be connected to the poleward motion of the absorption spikes (see Fig. 5). During 0732 UT–0736 UT while the third absorption spike was observed, the flow vectors rotated clockwise with high velocity in the higher-latitude cusp. This plasma vortex corresponds to the high-latitude cusp-aurora detached from the afternoon main oval in the POLAR UVI images (Fig. 6), associated with the lobe reconnection (Milan *et al*., 2000).

Consequently, the present absorption would be related to the relatively high velocity flows near the convection reversal of the convection cell, which is consistent with the result by Stauning and Rosenberg (1996). This suggests that absorption mechanism could be related to FAC enhanced near the convection reversal. However, a different point with Stauning and Rosenberg (1996) is that the strong magnetic compression may generate stronger FAC. Therefore the absorption spikes could be grown up to larger intensity and longer time-duration than the characteristics obtained by Stauning and Rosenberg (1996).

We suggest the solar wind-magnetosphere-ionosphere coupling mode for the present absorption spikes from the above discussions: The pressure increase of solar wind could stimulate strong magnetic compression at the northern hemisphere side near the dayside magnetopause. The strong magnetic compression could generate perturbations in the closed magnetic field lines and then produce Alfvén pulses in the inner edge of the magnetopause, inducing strong upward region 1 FAC. The upward FAC near the convection reversal could convey magnetospheric electrons (< 2 keV) from the LLBL region into the lower-latitude boundary of the cusp, producing the absorption in the E-region ionosphere. Recent statistical analysis of magnetic data from the low-altitude polar orbiting Ørsted satellite demonstrated the existence of strong upward FAC at the cusp-latitude under the conditions of IMF $B_z > 0$ and $B_y > 0$ (Vennerstrøm *et al*., 2002), which could suggest the absorption mechanism relating to upward FAC during the strong northward IMF.

5. Conclusion

Pre-noon ionospheric absorption spikes on August 26, 1998 observed by the inter-hemispheric IRISs in the cusp-latitude were presented. The conjugate absorption spikes were associated with the increase of the solar wind dynamic pressure during the strong northward IMF. This IMF condition is clearly different with the one on the previous absorption spike events on November 22, 1997 (Nishino *et al*., 2000). The absorption spikes showed intensity of < 1 dB and duration of 5–10 min. The absorption showed a larger spatial extension (> 400 km) exceeding the FOV of the IRIS. The conjugate relationship of the present absorption shows a good coincidence with the conjugate locations calculated by the T95-model. The absorption at NAL was situated at the enhanced auroral luminosity in the main oval from the Polar UV images. Electron precipitation of < 2 keV energies from the LLBL was simultaneously observed by the DMSP satellite flying near NAL. The absorption at NAL was located near the lower-latitude convection reversal at the plasma convection cell from the simultaneous SuperDARN network data. It is thus indicated that the increase of the solar wind pressure cause perturbations on the closed field lines at the dayside magnetopause, inducing strong upward region 1 FAC in the pre-noon hour. The strong upward FAC would convey magnetospheric electrons (< 2 keV) from the LLBL into the inter-

hemispheric *E*-region cusp-ionosphere. We will further examine ground magnetic perturbations caused by ionospheric currents using magnetic chain data around the IRIS stations.

Acknowledgments

We gratefully acknowledge the Norwegian Polar Research Institute and Chinese Antarctic Expedition for incessant IRIS observations at Ny-Ålesund and Zhongshan, respectively. We acknowledge Ron Lepping and K.W. Ogilvie, NASA Goddard Flight Center for the use of WIND MFI/SWE data, and P.T. Newell, Johns Hopkins University for the use of DMSP data. We obtained the plasma convection map from the SuperDARN network data using the analysis program of Communication Research Laboratory (CRL), to which we acknowledge.

The editor thanks Drs. K. Makita and T.J. Rosenberg for their help in evaluating this paper.

References

Brown, R.R. (1973): Sudden commencement and sudden impulse absorption events at high latitudes. J. Geophys. Res., **78**, 5698–5702.

Brown, R.R. (1977): Sudden commencement absorption events at the edge of the polar cap. J. Geophys. Res., **82**, 2433–2435.

Christensen, T., Ostgaard, N., Rosenberg, T., Detrick, D.L., Germany, G.A. and Stauning, P. (2003): Conjugate high-intensity energetic electron precipitation at high latitude. Ann. Geophys., **21**, 1443–1455.

Detrick, D.L. and Rosenberg T.J. (1990): A phased-array radiowave imager for studies of cosmic noise absorption. Radio Sci., **25**, 325–338.

Farrugia, C.J., Freeman, M.P., Cowley, S.W.H. and Southwood, D.J. (1989): Pressure-driven magnetopause motions and attendant response on the ground. Planet. Space Sci., **37**, 589–607.

Farrugia, C.J., Sandholt, P.E., Cowley, W.H., Southwood, D.J., Egeland, A., Stauning, P., Lepping, R.P., Lazarus, A.J., Hansen, T. and Friis-Christensen, E. (1995): Reconnection-associated auroral activity stimulated by two types of upstream dynamic pressure variations: Interplanetary magnetic field B_z~0, $B_y \ll 0$ case. J. Geophys. Res., **100**, 21753–21772.

Glassmier, K.H. and Heppner, C. (1992): Traveling magnetospheric convection twin vortices: Another case study, global characteristics and a model. J. Geophys. Res., **97**, 3977–3992.

Hargreaves, J.K. and Chivers, H.J.A. (1965): A study of auroral absorption events at the South Pole. 2. Conjugate properties. J. Geophys. Res., **70**, 1093–1102.

Milan, S.E., Lester, M., Cowley, S.W.H. and Brittnacher, M. (2000): Dayside convection and auroral morphology during an interval of northward interplanetary magnetic field. Ann. Geophys., **18**, 436–444.

Newell, P.T. and Meng, C.-I. (1992): Mapping the dayside ionosphere to the magnetosphere according to the particle precipitation characteristics. Geophys. Res. Lett., **19**, 609–612.

Newell, P.T. and Meng, C.-I. (1994): Ionospheric projections of magnetospheric regions under low and high solar wind pressure conditions. J. Geophys. Res., **99**, 273–286.

Nishino, M., Tanaka, Y., Oguti, T., Yamagishi, H. and Holtet, J.A. (1993): Initial observation results with imaging riometer at Ny-Ålesund (L=16). Proc. NIPR Symp. Upper Atmos. Phys., **6**, 47–61.

Nishino M., Yamagishi, H., Sato, N., Liu, R., Hu, H., Stauning, P. and Holtet, J. (2000): Conjugate features of daytime absorption associated with specific changes in the solar wind observed by inter-hemispheric high-latitude imaging riometers. Adv. Polar Upper Atmos. Res., **14**, 76–92.

Nishino, M., Yamagishi, H., Sato, N., Murata, Y., Liu, R., Stauning, P. and Holtet, J. (2001): Conjugate imaging riometer observations at polar cusp/cap stations: A daytime absorption event for specific change of the solar wind conditions. Mem. Natl Inst. Polar Res., Spec. Issue, **54**, 29–41.

Ruohoniemi, J.M. and Baker, K. B. (1998): Large-scale imaging of high-latitude convection with SuperDARN HF

radar observations. J. Geophys. Res., **103**, 20797–20811.

Sandholt, P.E., Farrugia, C.J., Burlaga, L.F., Holtet, J.A., Moen, J., Lybekk, B., Jacobsen, D., Opsvik, D., Egeland, A., Lepping, R., Lazalus, A.J., Hansen, T., Brekke, A. and Friis-Christensen, E. (1994): Cusp/cleft auroral activity in relation to solar wind dynamic pressure, interplanetary magnetic field B_z and B_y. J. Geophys. Res., **99**, 17323–17342.

Sandholt, P.E., Farrugia, C.J., Stauning, P., Cowley, S.W.H. and Hansen, T. (1996): Cusp/cleft auroral forms and activities in relation to ionospheric convection: Response to specific changes in solar wind and IMF conditions. J. Geophys. Res., **101**, 5003–5020.

Sandholt, P.E., Farrugia, C.J., Cowley, W.H., Lester, M., Denig, W.F., Cerisier, J.-C., Milan, S.E., Trondsen, E. and Lybekk, B. (2000): Dynamic cusp aurora and associated pulsed reverse convection during northward interplanetary magnetic field. J. Geophys. Res., **105**, 12869–12894.

Sato, M., Yamagishi, H., Kato, Y. and Nishino, M. (1992): Quick-look system of auroral absorption images by imaging riometer. Nankyoku Shiryô (Antarct. Rec.), **36**, 251-267 (in Japanese with English abstract).

Sato, N., Nagaoka, T., Hashimoto, K. and Saemundsson, T.H. (1998): Conjugacy of isolated auroral arcs and nonconjugate auroral breakups. J. Geophys. Res., **103**, 11641–11652.

Sibeck, D.G., Baumjohann, W. and Lopez, R.E. (1989a): Solar wind dynamic pressure variations and transient magnetopsheric signatures. Geophys. Res. Lett., **16**, 13–16.

Sibeck, D.G., Baumjohann, W., Elphic, R.C. Fairfield, D.C., Fennel, J.F., Gail, W.B., Lanzerotti, L.J., Lopez, R.E., Luhr, H., Lui, A.T.Y., Maclenann, C.G., McEntire, R.W., Potemra, T.A., Rosenberg, T.J. and Takahashi, K. (1989b): The magnetospheric response to 8-min period strong-amplitude upstream pressure variation. J. Geophys. Res., **94**, 2505–2519.

Stauning, P. (1996): Investigations of ionospheric radio wave absorption processes using imaging riometer techniques. J. Atmos. Terr. Phys., **58**, 753–764.

Stauning, P. and Rosenberg, T.J. (1996): High-latitude daytime absorption spike events. J. Geophys. Res., **101**, 2377–2396.

Stauning, P., Clauer, C.R., Rosenberg, T.J., Friis-Christensen, E. and Sitar, R. (1995): Observations of solar-wind-driven progression of interplanetary magnetic field B_y-related dayside ionospheric disturbances. J. Geophys. Res., **100**, 7567–7585.

Torr, M.R., Torr, D.G., Zukic, M., Johnson, R.B., Ajello, J., Banks, P., Clark, K., Cole, K., Keffer, C., Parks, G., Tsurutani, B. and Spann, J. (1995): A far ultraviolet imager for the international solar-terrestrial physics mission. Space Sci. Rev., **71**, 329.

Vennestrøm, S., Moretto, T., Olsen, N., Friis-Christensen, E. and Stampe, A.M. (2002): Field-aligned currents in the dayside cusp and polar cap region during northward IMF. J. Geophys. Res., **107**(A8), doi:10,1029/2001JA009162.

Yamagishi, H., Nishino, M., Sato, M., Kato, Y., Kojima, M., Sato, N. and Kikuchi, T. (1992): Development of imaging riometers. Nankyoku Shiryô (Antarct. Rec.), **36**, 227–250 (in Japanese with English abstract).

Yamagishi, H., Fujita, Y., Sato, N., Stauning, P., Nishino, M. and Makita, K. (1998): Conjugate features of aurora observed by TV camera and imaging riometers at auroral and polar cap conjugate pair stations. Polar Cap Boundary Phenomena, ed. by J. Moen *et al*. Doerdrecht, Kluwer, 289–300 (NATO ASI Ser.; C-509).

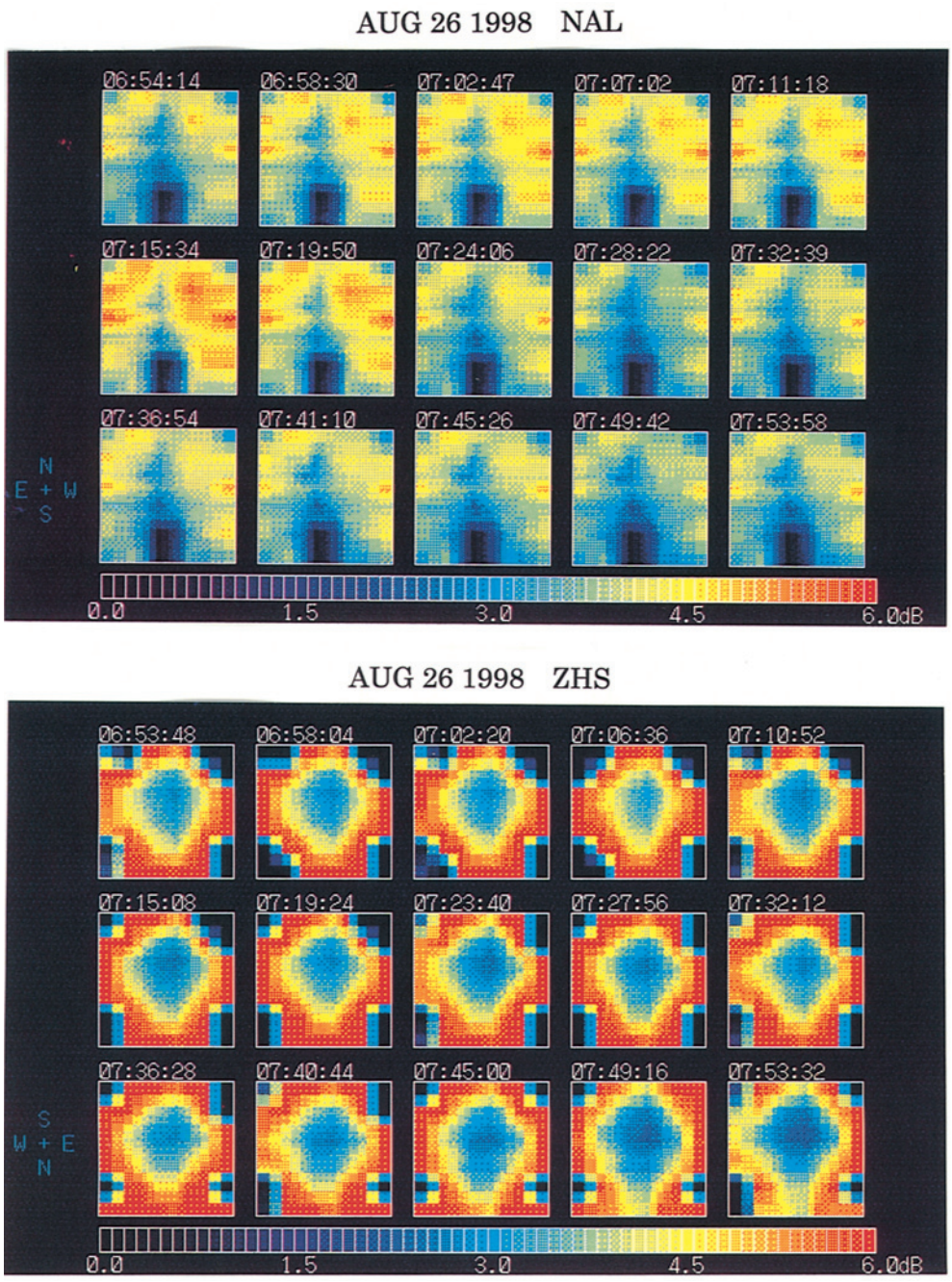

Plate 1. Time series of absorption image data during about 0654–0754 UT at NAL (upper panel) and ZHS (lower panel). The both images are composed from the two-dimensional 8 × 8 beam data (Sato et al., 1992). The absorption intensity is displayed by color codes below the image data.

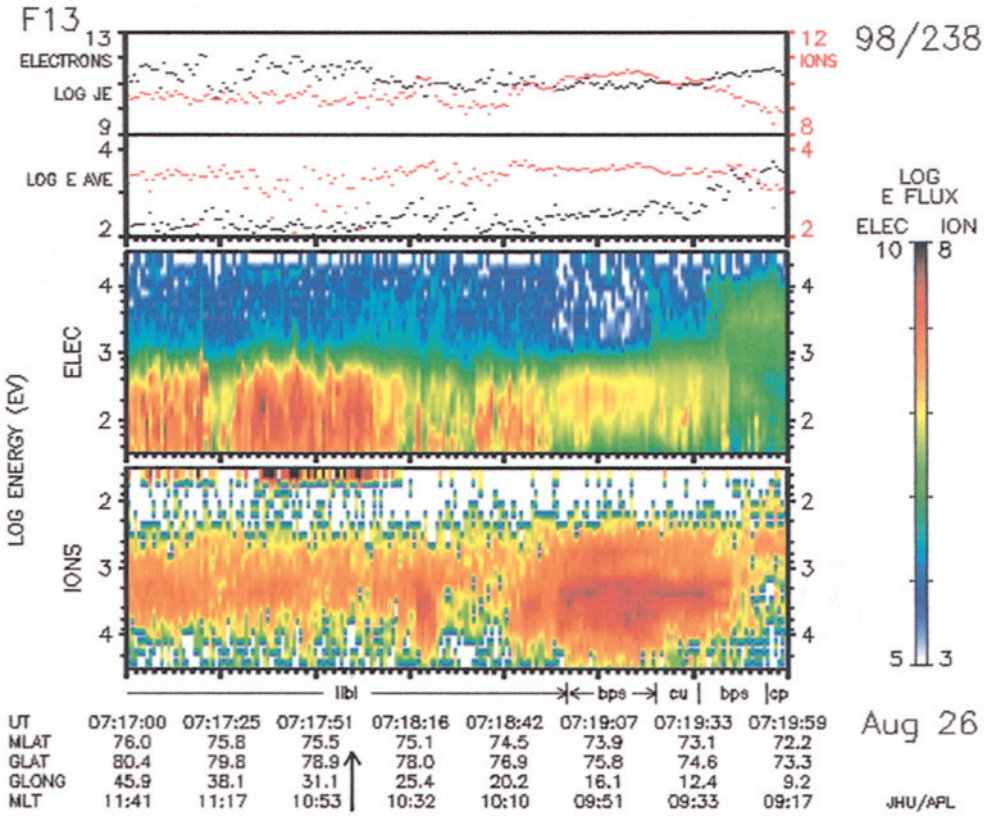

Plate 2. Spectrograms of energetic particle (electrons and ions) precipitations with UT, MLAT, GLAT, GLONG and MLT on August 26, 1998.

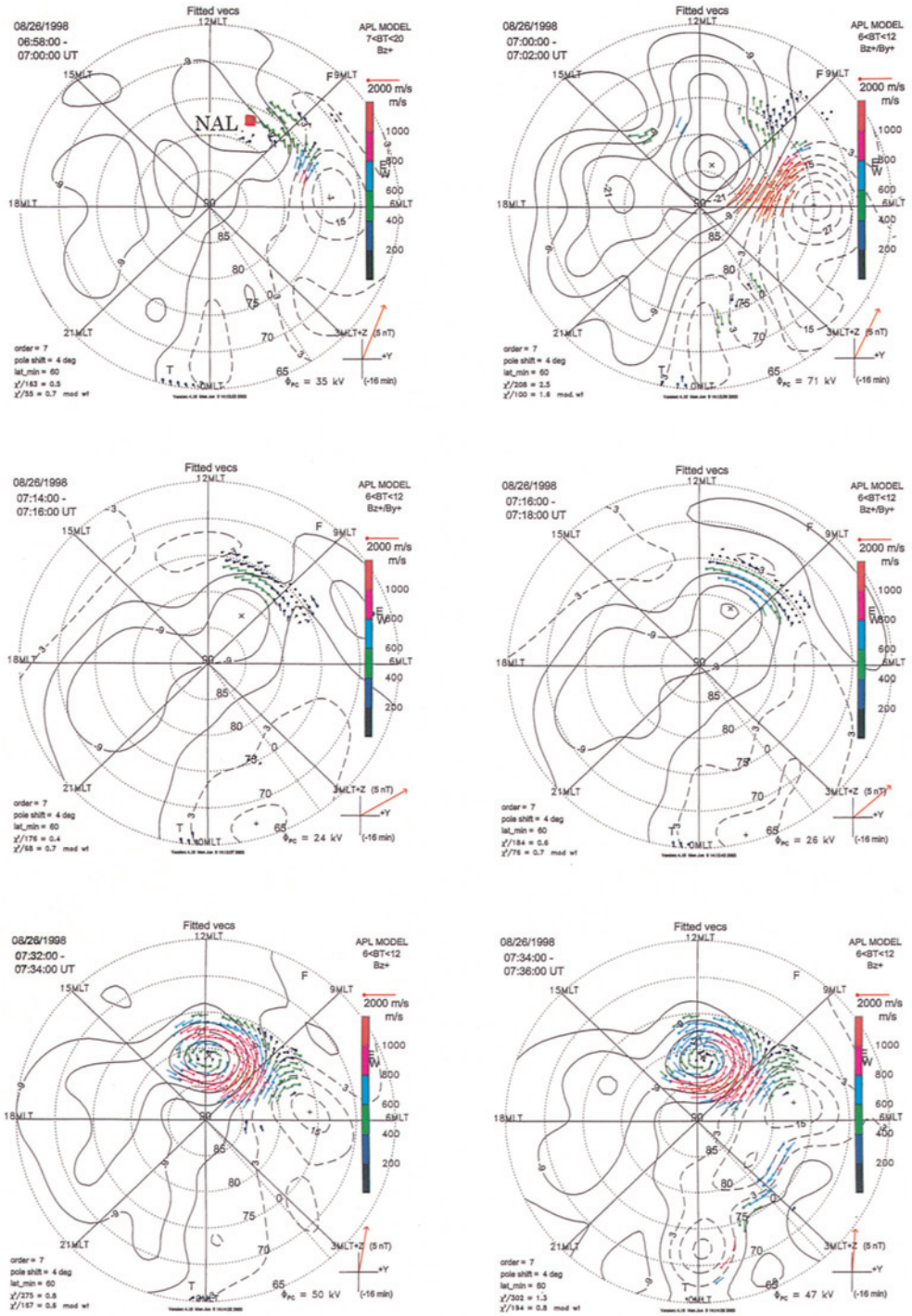

Plate 3. Ion flow vector plots in northern polar region on the 2 min durations from 0658 UT, 0700 UT, 0714 UT, 0716 UT, 0732 UT and 0734 UT (approximately 1030–1100 MLT) when the absorption spikes were observed. The flow vectors are plotted in MLT/MLAT coordinates.